PRAMANA
— journal of
physics

Vol. 71, No. 4
October 2008
pp. 877–885

Small-angle neutron scattering study of structural evolution of different phases in protein solution

V K ASWAL[1,*], S CHODANKAR[1], J KOHLBRECHER[2], R VAVRIN[2] and A G WAGH[1]

[1]Solid State Physics Division, Bhabha Atomic Research Centre, Mumbai 400 085, India
[2]Laboratory for Neutron Scattering, ETH Zurich & Paul Scherrer Institut, CH-5232 Villigen PSI, Switzerland
[*]Corresponding author. E-mail: vkaswal@barc.gov.in

Abstract. Small-angle neutron scattering (SANS) has been used to study the structural evolution of different phases in protein solution leading to crystallization, denaturation and gelation. The protein solution under crystallization mostly consists of monomers and dimers, and higher-mers are not observed as they are perhaps formed in very small numbers. The onset and the rate of crystallization strongly depend on the salt concentration. Protein denaturation on addition of surfactant occurs due to the formation of micelle-like clusters along the unfolded polypeptide chains of the protein. The structure of such protein–surfactant complex is found to be independent of the size of the micelles in their pure surfactant solutions. The structure of temperature-induced protein gels shows a fractal structure. Rheology of these gels shows a strong dependence on varying pH or protein concentration, whereas the structure of such gels is found to be similar.

Keywords. Small-angle neutron scattering; biological macromolecules; protein solution.

PACS Nos 61.12.Ex; 87.14.Ee; 87.15.Nn

Biological macromolecules such as proteins possess a specific shape and charge, which regulate and control the functionality and stability of these molecules. Proteins in aqueous solution are known to interact through different interaction forces. These forces are involved in controlling macromolecular solubility and organization, in addition to governing liquid–liquid phase separation, crystal growth, or any separated protein phases [1]. Different phases in any protein solution are preceded and followed by structural changes among them, which can be induced simply by increasing temperature and neutralizing the charge on the macromolecules or breaking the water structure, and can be initiated by additives such as salt or surfactant. The possibility to vary scattering contrast either by deuterating the particle or solvent makes small-angle neutron scattering (SANS) a unique technique to characterize the hydrogenous protein systems [2]. Herein, we present some of our recent results of SANS study of structural evolution of different phases leading to crystallization, denaturation and gelation in protein solution.

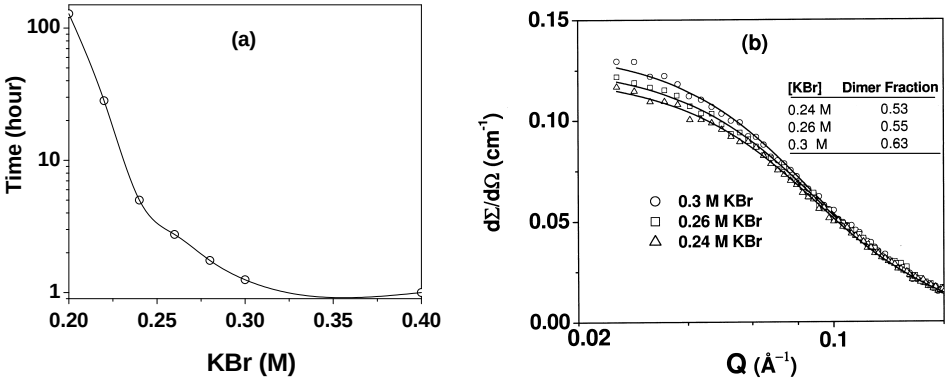

Figure 1. (**a**) Phase diagram of crystallization of 1 wt% lysozyme in the presence of varying KBr concentration and (**b**) SANS data for 1 wt% lysozyme for three KBr concentrations.

Lysozyme and BSA proteins, surfactant SDS and salt KBr were purchased from Fluka. The samples for SANS experiments were prepared by dissolving known amounts of BSA, lysozyme and additives in D_2O. The use of D_2O as solvent instead of H_2O provides better contrast in neutron experiments. Small-angle neutron scattering experiments were performed on the SANS instrument at the Dhruva reactor, Bhabha Atomic Research Centre, Mumbai [3] and at Swiss Spallation Neutron Source, SINQ, Paul Scherrer Institut, Switzerland [4]. In particular, the lower concentrations of protein and the time-resolved measurements were performed at the SINQ SANS instrument because of the high signal-to-background ratio of this instrument. SANS data were corrected and normalized to a cross-sectional unit using standard procedures.

1. Crystallization of lysozyme

Growing protein crystals for structure determination using crystallography techniques is still an intriguing task. The process requires that the concentration of solute in the solution exceeds the solubility limit, which is also known as supersaturation stage. Structural evolution among protein macromolecules is an important step in understanding the process that the system is undergoing during crystallization. The onset and rate of protein crystallization is principally determined by the mechanism of molecular incorporation among the macromolecules. Self-association of protein macromolecules in a periodic array to form crystals or any other separated phase is governed by the interaction among them, caused predominantly due to the presence of charge on the protein macromolecules. The charge on the macromolecule and so the interaction among them can be controlled by the addition of salt or some other additives [5]. It is thus possible to tune the interactions among the macromolecules in order to achieve specific phase transformations.

Figure 1a shows the phase diagram of crystallization of 1 wt% lysozyme protein solution as a function of KBr concentration. It is observed that as the concentration

of KBr is increased, the onset time of crystallization in protein solution decreases. At low KBr concentrations, the protein solution has an asymptotic time dependence on the occurrence of crystallization. For example, while 0.2 M KBr shows crystals in protein solution in about 120 h, it is reduced to only 5 h in the presence of 0.24 M KBr. On further increase in salt concentration, crystallization time shows much slower dependence on the salt. The crystallization time is reduced from 5 h to 1 h as the salt concentration increases from 0.24 to 0.4 M KBr. It has been visually observed that rate of crystallization strongly depends on the onset of crystallization in protein solution as controlled by the salt concentration. The rate of crystallization has been quantitatively measured using SANS for three protein solutions having KBr concentrations 0.24, 0.26 and 0.3 M, which show the onset of crystallization at about 5, 3 and 1.5 h, respectively. The rate of crystallization in these systems has been measured up to 72 h.

SANS data on freshly prepared 1 wt% lysozyme in the presence of 0.24, 0.26 and 0.3 M KBr are shown in figure 1b. The low concentration of lysozyme and high concentration of salt have been used to minimize the interaction between charged protein macromolecules. The analysis suggests that protein solution mostly consist of monomers and dimers [6]. The monomers of the protein macromolecules have been found to be prolate ellipsoidal with dimensions of semi-major and semi-minor axes as 22.0 $\pm$ 1.0 and 13.5 $\pm$ 0.5 Å, respectively. The dimer fraction increases with the increase in the salt concentration. The calculated fractions of dimers are given in the inset of figure 1b. These results thus suggest that in addition to the difference in ionic strength, the protein solutions in the presence of 0.24, 0.26 and 0.3 M KBr also have the differences in their structures in terms of the populations of monomers and dimers.

Time-resolved SANS data in 1 wt% lysozyme in the presence of 0.24 M KBr during crystallization are shown in figure 2a. The formation of small crystals in this sample starts in about 5 h. The SANS data were recorded in every 1 h up to 72 h. Figure 2a shows data measured every 4 h. It is interesting to note that there is no significant change up to 5 h when the crystallization has already started in the protein solution. This observation suggests that protein solution at crystallization still consists of monomers and dimers as present in the freshly prepared sample and fraction of monomers and dimers that leads to crystallization is very small. The scattering intensity decreases with time only after some time of the start of crystallization. Thereafter the decrease in scattering intensity increases with crystallization time, which finally saturates at higher times. The fact that features of scattering profile do not change during crystallization suggest that even after a long time after the crystallization starts, the protein solution mostly consists of monomers and dimers. Higher-mers that lead to crystallization are not observed in the solution. This is possible if the higher-mers, including nucleated structures are formed in very small numbers in the process towards the crystallization. The scaling of the data after correcting for incoherent background from the sample is shown in the inset of the figure.

The variation of crystallization fraction as a function of time for 1 wt% lysozyme in the presence of 0.24, 0.26 and 0.3 M KBr is shown in figure 2b. It is seen that these protein solutions showing the start of crystallization at different times as controlled by salt concentration have very different crystallization rate over a period

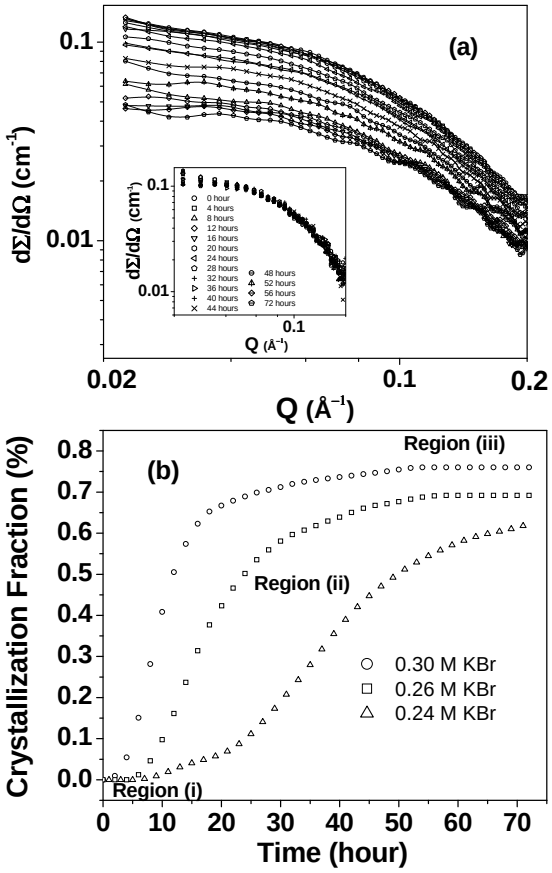

Figure 2. (**a**) Time-resolved SANS data of 1 wt% lysozyme with 0.24 M KBr and (**b**) measured crystallization fraction for 1 wt% lysozyme with three KBr concentrations.

of time [7]. Each curve mainly consists of three regions: (i) prior to crystallization, where there is no significant change in the crystallization, (ii) the growth region of crystallization for which the fraction of crystallization increases with the time and (iii) saturation region of the crystallization. The initial start of the crystallization is slow for the samples where the start of crystallization is longer. The slope of crystallization in the growth region is also small when the time of crystallization is longer. The saturation takes much longer time for the samples for which the crystallization occurs late.

2. Surfactant-induced protein denaturation

Both the ionic surfactant and protein in aqueous solution share the common property of having charged groups and hydrophobic portions. It is believed that in a

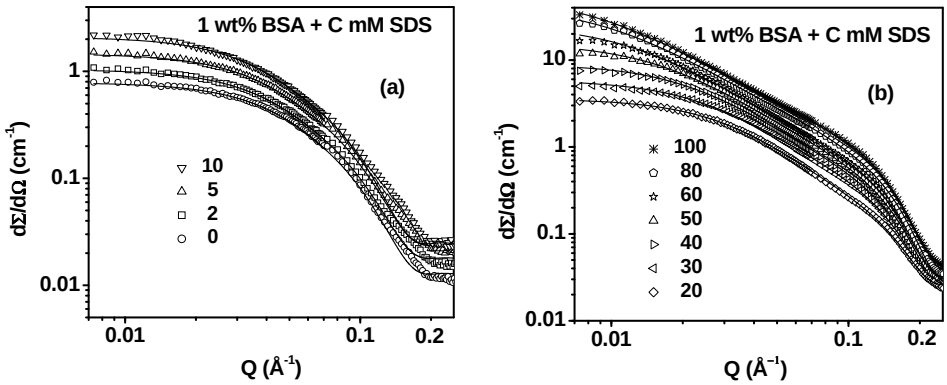

Figure 3. SANS data for 1 wt% BSA with varying SDS concentrations. (**a**) Low SDS concentrations and (**b**) high SDS concentrations.

system consisting of these two components, surfactant molecules at low concentrations undergo electrostatic binding to the protein, whereas above critical aggregation concentration hydrophobic interaction amongst surfactant molecules takes over the binding process [8]. At higher surfactant concentrations, the binding of surfactants to the protein macromolecules leads to their denaturation, which is considered as the surfactant-induced unfolding of the protein. Understanding the behaviour of such protein–surfactant complexes is of vital interest and allows to gain insight into the binding mechanism between the two components and its effect on the protein structure and function in the complex.

SANS data for 1 wt% BSA in the presence of varying SDS concentration are shown in figure 3. Based on the features of the scattering profiles, the data can be grouped in two different sets as the surfactant concentration is increased [9]. The first dataset corresponds to proteins at low surfactant concentrations (0 to 10 mM), where the scattering data show similar behaviour to that of pure protein solution (figure 3a). In this dataset, the overall scattering cross-section increases with increase in surfactant concentration. It can be explained if the individual surfactant molecule binds to protein and the volume of the scattering particle increases. The features of the scattering data in the second dataset at higher surfactant concentrations (>10 mM) are very different (figure 3b) from those of the first dataset (figure 3a). One interesting feature is the linearity of the scattering profiles on log–log scale in the intermediate Q range with the Q range of linearity increasing with surfactant concentration. This is an indication of the formation of fractal structure by the protein–surfactant complex [10]. The fractal dimension of the complex decreases from 2.27 to 1.71 on increasing the surfactant concentration from 20 to 100 mM. The build-up of scattering cross-section in the higher cut-off of the linearity of scattering data suggests the formation of micelle-like surfactant aggregates and the lower cut-off corresponds to the overall size of the protein–surfactant complex. It is observed that the position of high Q cut-off remains almost same while the position of low Q cut-off shifts to smaller Q values with increasing surfactant concentration.

SANS data on 1 wt% SDS micellar solution in the presence of 0.5 M concentration of salts LiBr, NaBr and 1 : 1 mixture of LiBr and NaBr are shown in figure 4a. The

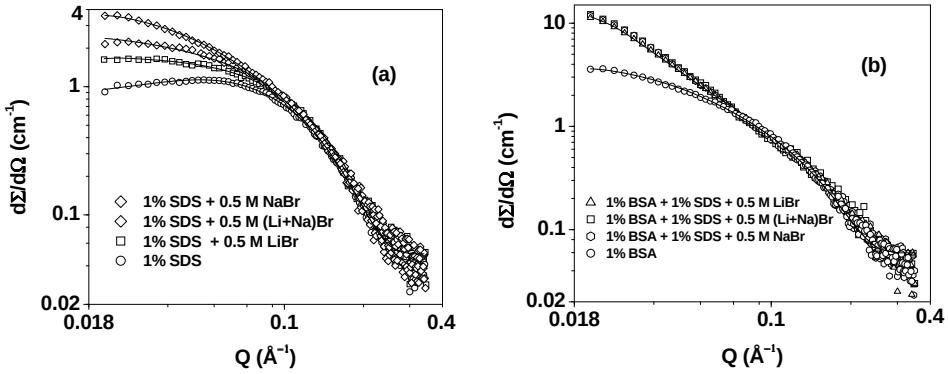

Figure 4. SANS data of (**a**) 1 wt% SDS with different salts and (**b**) 1 wt% BSA with 1 wt% SDS at different salts.

scattering intensity in the low Q region increases with the addition of salt, which is an indication of increase in the size of micelles. The micellar solution of 1 wt% SDS in the absence of salt forms ellipsoidal micelles. On addition of salts, the micellar size increases and the fractional charge decreases. It is found that the increase in micellar size is much larger in 0.5 M NaBr than that in 0.5 M LiBr. The effect of mixture of the two salts lies in between that of LiBr and NaBr. The difference in the addition of LiBr and NaBr on the size of the micelle occurs because of the fact that the hydrated sizes of Li^+ and Na^+ counterions are different [11]. Figure 4b depicts the SANS data on addition of 1 wt% BSA with the micellar solutions as shown in figure 4a. The scattered intensity on addition of protein to the micelle solution varies linearly on log–log scale in about one order Q range, which suggests the formation of fractal structure in protein–surfactant complexes. It is found that irrespective of different sizes of micelles formed in their pure solutions, these micelles in the presence of proteins show identical fractal structure on the formation of protein–surfactant complexes [12].

3. Temperature-induced protein gelation

Heat-induced protein gelation is believed to be due to hydrophobic groups in protein, which at ambient temperature remains buried inside the protein, becomes exposed to water at higher temperatures [13]. This hydrophobic effect leads to aggregation to form networks of protein gel. The phase diagrams of protein gelation temperature as a function of pH and protein concentration are shown in figure 5a. The phase diagram for the effect of pH is shown for 1 wt% protein solution in the pH range of 5 to 8.5. The gelation temperature is found to increase systematically as the pH is increased. For example, at pH 5 the gelation temperature is 62°C, and it rises to 94°C on increasing the pH to 8.5. This increase in gelation temperature can be understood on the basis of the change in the net charge on a protein macromolecule as the pH is varied. The BSA protein has an isoelectric pH at about 4.7, where the net charge is close to zero and on increasing the pH away from isoelectric point the net charge on a protein macromolecule increases. To overcome this

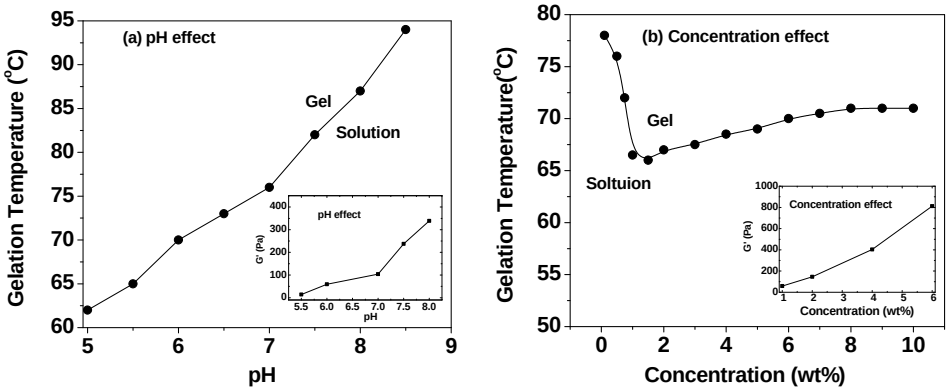

Figure 5. Temperature-induced phase diagram of protein gelation. (**a**) Effect of varying pH for 1 wt% BSA and (**b**) effect of concentration at constant pH of 5.5. Insets show the variation of storage modulus of the gels with pH or concentration.

increased electrostatic force of repulsion at pH values away from isoelectric point a larger driving force is required to bring these molecules closer to undergo aggregation and gelation. The driving force in this case is provided to avoid increasing exposure of hydrophobic patches at higher temperatures, which causes increase in hydrophobic force of attraction. Figure 5b shows the phase diagram of the effect of varying protein concentration (0.1 to 10 wt%) at fixed pH 5.5. Usually, it is found in the literature that the protein gelation temperature decreases with increase in concentration. However, we observe that in the case of BSA protein the decrease in gelation temperature in the low concentration regime is followed by a small increase in gelation temperature at higher protein concentrations. The decrease in gelation temperature is understood in terms of decreasing solubility of the system with increasing concentration and also indicates a critical concentration only above which a gel can be formed. It is not clear why the gelation temperature for protein BSA increases at higher protein concentrations. The insets of figure 5 show the rheological data on protein gels at various pH values and concentrations. The data points display only the storage modulus (G') measured at angular frequency of 1 Hz as a function of pH. The storage modulus represents the elastic component of the viscoelastic properties of the gels. It is found that there is increase in storage modulus on increasing the pH away from isoelectric pH. This increase in storage modulus can be associated to the increase in the net charge on the protein macromolecules with shift in pH from isoelectric point. It is also found that there is a large increase in storage modulus on increasing the protein concentration in the solution. The increase in storage modulus is believed to be due to increase in protein number density with increasing protein concentration leading to stronger networking.

SANS data for protein gels prepared at different pH are shown in figure 6a. The scattered intensity shows a linear region on log–log scale for values of $Q < 0.07$ Å^{-1}. This represents the fractal structure of gels as characterized by the network kind of arrangement of protein aggregation in the system [14]. Interestingly, the SANS data

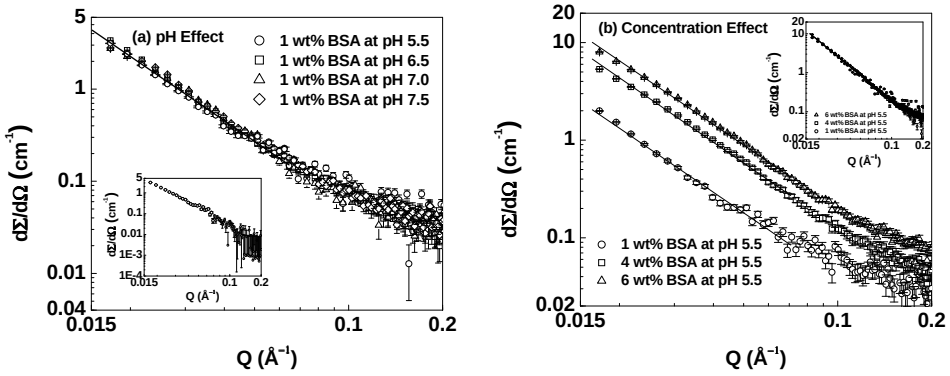

Figure 6. SANS data of protein gels of 1 wt% BSA prepared at (**a**) different pH and (**b**) different protein concentrations.

profile for various pH are similar, although there is a large variation in their values of storage modulus (figure 5). Inset of the figure shows the data after correcting for incoherent background. Fractal dimension for all the gels is found from the slope of the linear region, which has a value of about 2.2. This suggests that although the physical structure of the protein gels is quite similar to one another, it can correspond to very different rheological properties at different pH values. The difference in the structural and rheological properties can be attributed as if the flocs in the gels which undergo networking have similar structure but different flexibility. The structure of flocs depends on the branching of the aggregation and the flexibility is decided by the charge on the flocs which at present has been varied by the change in pH value.

SANS data for protein gels prepared at different protein concentrations and at fixed pH value of 5.5 are shown in figure 6b. It is found that on increasing the protein concentration there is substantial increase in scattering intensity in the overall Q range. However, scattering cross-section profiles have similar features irrespective of the protein concentration. This is also verified by scaling the data (inset of figure 6b). The data match very well on scaling, indicating that the arrangement of protein macromolecules in the aggregates is similar for all the protein concentrations. The fractal dimension for the protein gels for different protein concentrations (1, 4 and 6 wt%) has same value of 2.2. The correlation of rheology (figure 5) and gel structure of protein can be understood when the structural arrangements in the flocs remains similar, whereas the number density of such flocs increases leading to larger hindrance to the flow property and subsequent increase in storage modulus.

In conclusion, SANS has been used to characterize the evolution of protein structure during different phases that leads to crystallization, denaturation and gelation. It has been shown that the crystallization rate strongly depends on salt concentration. Surfactant-induced denaturation occurs due to formation of micelle-like surfactant clusters along the unfolded polypeptide chain. The elastic properties of temperature-induced protein gels are very different with varying pH and concentration, whereas they show similar fractal structure.

References

[1] R Piazza, *Curr. Opin. Colloid Interface Sci.* **5**, 38 (2000)
[2] D I Svergun and M H J Koch, *Rep. Prog. Phys.* **66**, 1735 (2003)
[3] V K Aswal and P S Goyal, *Curr. Sci.* **79**, 947 (2000)
[4] J Kohlbrecher and W Wagner, *J. Appl. Crystallogr.* **33**, 804 (2000)
[5] A Stradner, H Sedgwick, F Cardinaux, W C K Poon, S U Egelhaaf and P Schurtenberger, *Nature (London)* **432**, 492 (2004)
[6] S Chodankar and V K Aswal, *Phys. Rev.* **E72**, 041931 (2005)
[7] S Chodankar, V K Aswal, J Kohlbrecher, P A Hassan and A G Wagh, *Physica* **B398**, 164 (2007)
[8] E D Goddard and K P Ananthapadmanabhan, *Interaction of surfactants with polymers and proteins* (CRC Press, London, 1993)
[9] S Chodankar, V K Aswal, J Kohlbrecher, R Vavrin and A G Wagh, *J. Phys.: Condens. Matter* **19**, 326102 (2007)
[10] X H Guo, N M Zhao, S H Chen and J Teixeira, *Biopolymers* **29**, 335 (1990)
[11] V K Aswal and P S Goyal, *Phys. Rev.* **E61**, 2947 (2000)
[12] S Chodankar, V K Aswal, P A Hassan and A G Wagh, *Physica* **B398**, 112 (2007)
[13] W S Gosal and S B Ross-Murphy, *Curr. Opin. Colloid Interface Sci.* **5**, 188 (2000)
[14] S Chodankar, V K Aswal, J Kohlbrecher, R Vavrin and A G Wagh, *Phys. Rev.* **E77**, 031901 (2008)